Good [morning/afternoon] everyone, and thank you for the opportunity to present our work. Today I will talk about the seismic design coefficients and failure mechanisms of composite concrete–steel structures that support air-cooled condenser (ACC) systems in power plants. This research was carried out by the Engineering Deputy team at MAPNA Group, MD1 Co., and focuses on a structural system that is widely used in Iranian thermal power plant projects but for which no dedicated seismic design provisions currently exist in national or international codes.

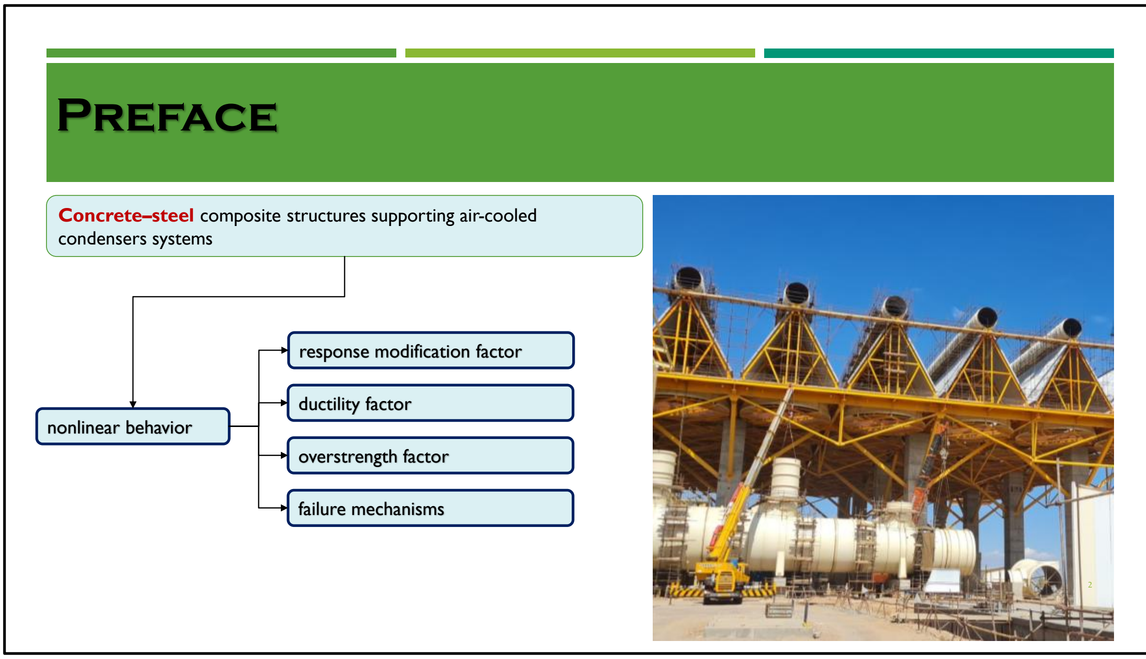

Preface

To set the stage, our study centers on concrete–steel composite structures that support air-cooled condenser systems. Because these structures often carry heavy, sensitive rotating equipment such as fans and motors at their top level, and because many power plants are located in seismically active regions, it is essential to understand their nonlinear seismic behavior. In this research we focus on four key outputs: the response modification factor (R), the ductility factor (μ), the overstrength factor (Ω_0), and the failure mechanisms, meaning the type, location, and progression of damage in these structures under lateral loading.

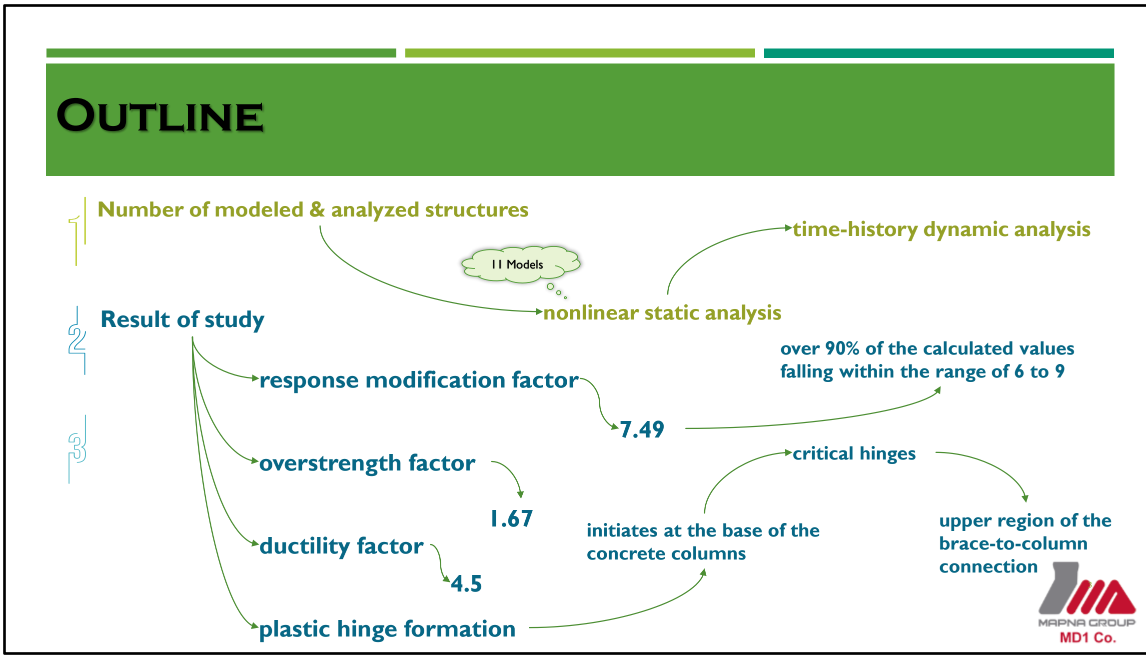

Outline

Let me briefly outline what we did and what we found. We developed and analyzed eleven full structural models representative of real ACC support structures used in Iranian power plant projects. Each model was subjected to nonlinear static (pushover) analysis in two orthogonal directions, and one representative model was additionally subjected to nonlinear time-history dynamic analysis. In terms of results, the average response modification factor obtained was 7.49, with more than 90% of all computed values falling between 6 and 9. The average overstrength factor was 1.67, and the average ductility factor was 4.5. Regarding failure mechanisms, plastic hinges first initiate at the base of the concrete columns, but the most critical hinges, those most likely to reach the collapse/failure limit, form in the upper region of the brace-to-column connection, a zone that plays a decisive role in overall structural stability.

Findings

The findings of this study can serve as a basis for revising seismic coefficients and improving design criteria for these structures in future power plant projects.

Objective of the Study

In thermal cyclic power plants, Cooling systems are responsible to condensate the steam and return it to the cycle.

Since the severe reduction of natural water resources and environmental criteria, ACC's which use the ambient atmosphere instead of water become an optimal and common cooling system in power plants.

Findings / Objective of the Study (Introduction)

Before going into the objective, let me give some context. In thermal and combined-cycle power plants, cooling systems are responsible for condensing the steam exiting the turbine and returning it as water to the process cycle. Traditionally, water-cooled condensers were used, but due to the severe reduction of natural water resources and increasingly strict environmental regulations, air-cooled condensers, which use ambient air and large fans instead of water, have become the preferred and increasingly common cooling solution in modern power plants. The findings of our study are intended to serve as a basis for revising seismic design coefficients and improving design criteria for these support structures in future power plant projects.

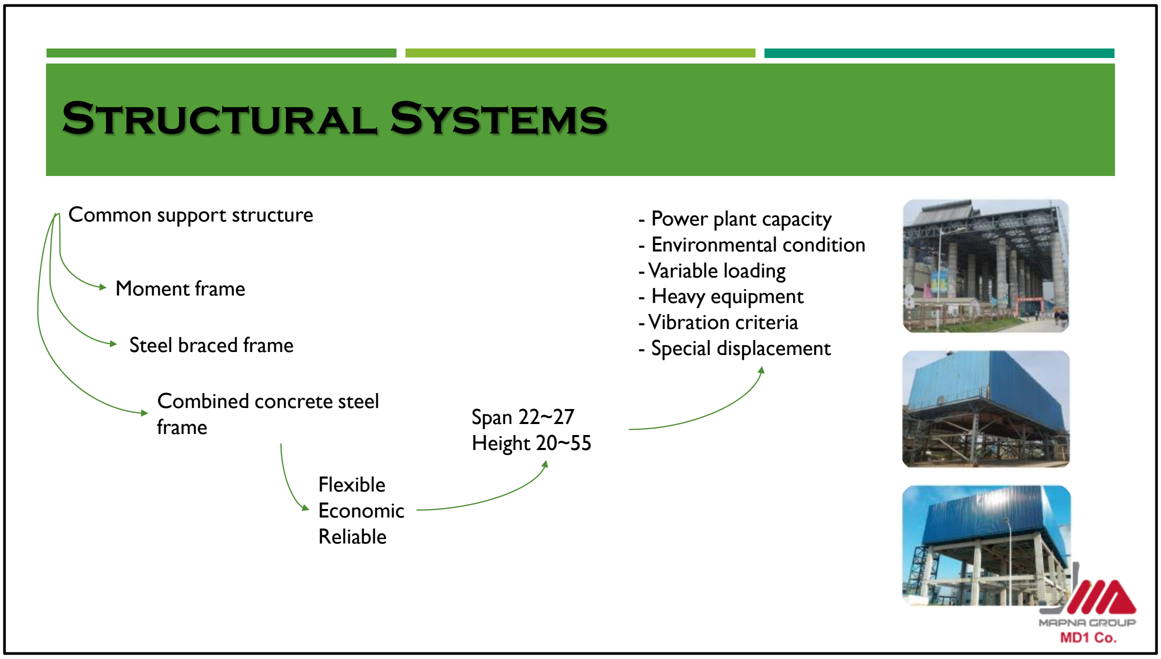

Objective of the Study (Structural Systems)

Several structural systems have historically been used to support ACC systems: reinforced concrete moment frames, steel braced frames, and combined concrete–steel frames. Among these, the combined concrete-steel frame, consisting of reinforced concrete hollow columns supporting steel girders or trusses, has become the preferred choice for many industrial and power plant projects because it offers a good balance of flexibility, economy, and reliability. These structures are typically designed with spans in the range of 22 to 27 meters and column heights between 20 and 55 meters, depending on several factors: the power plant's capacity, environmental conditions, variable operational loading, the weight and dynamics of the heavy fan equipment, vibration serviceability criteria, and special displacement requirements needed to protect the sensitive equipment mounted at the top of the structure.

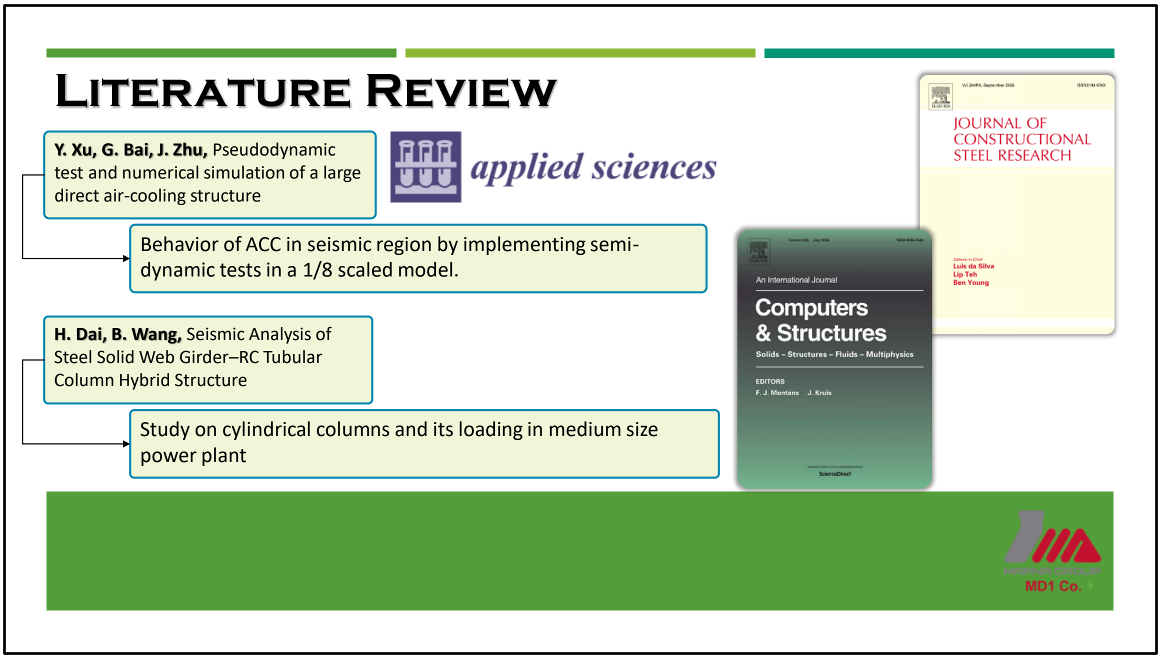

Major Studies (Literature Review)

Prior research on the seismic behavior of ACC support structures is limited but valuable. Xu, Bai, and Zhu carried out a pseudo-dynamic test and numerical simulation on a large direct air-cooling structure, evaluating its behavior in high-seismicity regions using a 1/8-scale single-span laboratory specimen subjected to five different peak ground acceleration levels; they found that with a ductility factor design value greater than 4, the system has adequate capacity to withstand seismic demands, and that steel truss and brace members mostly remained elastic throughout testing. Dai and Wang performed a full-scale numerical seismic analysis in ABAQUS of a steel solid-web-girder–RC tubular column hybrid structure, representative of medium-sized power plant applications, and found that damage concentrated in the reinforced concrete tubular columns, particularly near the column base and near the upper and lower corbel connection regions, while the steel members remained essentially elastic. These studies, along with others referenced in the paper (Wang et al., Yao and Lui), also highlighted that despite an approximately symmetric floor plan, ACC structures often exhibit significant torsional response due to uneven mass and stiffness distribution over their height, which existing seismic codes do not adequately address for this structural typology.

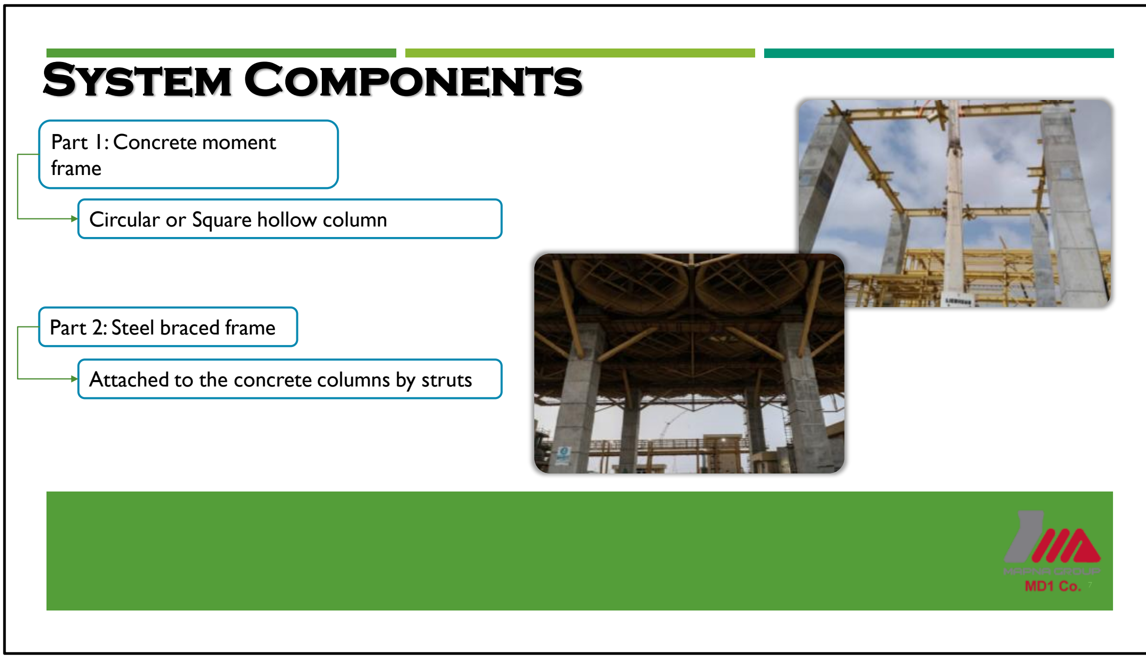

Combined Concrete Steel Frame (System Components)
Let's look more closely at the combined concrete–steel frame system that is the focus of this study. It consists of two main parts. The first part is the reinforced concrete moment frame, made up of circular or square hollow reinforced concrete columns, in Iranian power plant practice, square hollow sections are the common choice. The second part is the steel braced frame, comprising steel girders, intermediate beams, and an A-frame system supporting the fan deck; these steel elements are connected to the concrete columns through diagonal steel brace members, often referred to as "struts," which ensure integrated and coordinated performance of the concrete and steel parts during an earthquake.

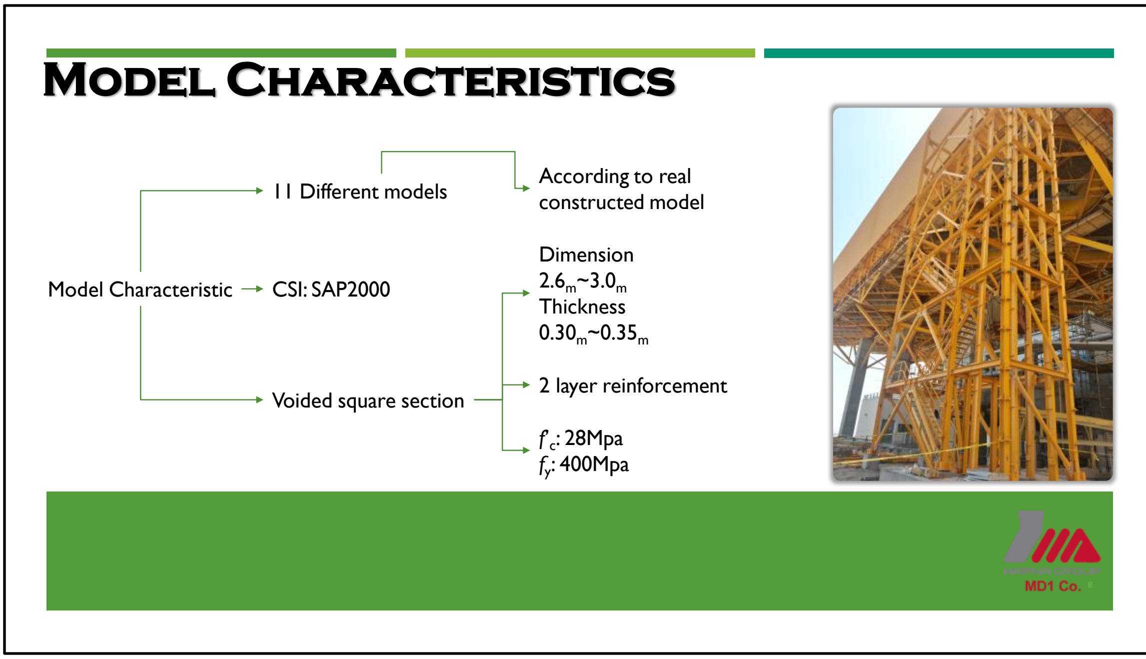

Combined Concrete Steel Frame (Model Characteristics)

For this study, we developed eleven different structural models based on the actual geometry, member sizes, and construction details of real ACC structures built in Iranian power plant projects, in accordance with the recommendations of FEMA P-695 for selecting a representative set of index archetype models. All models were built and initially analyzed in the SAP2000 software environment. The reinforced concrete columns use a voided (hollow) square cross-section, with side dimensions ranging from 2.6 to 3.0 meters and wall thickness between 0.30 and 0.35 meters, reinforced with two layers of longitudinal rebar in each wall. The material properties used were a concrete compressive strength of 28 MPa and a reinforcing steel yield strength of 400 MPa, while the structural steel members use a mild steel with a yield strength of 235 MPa.

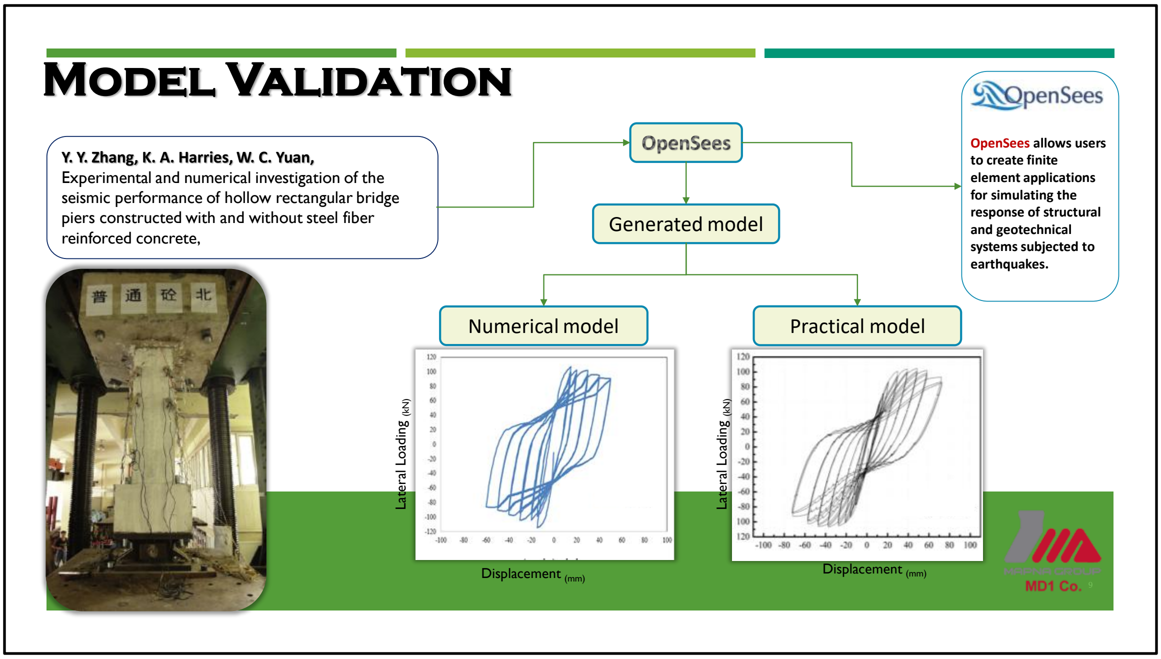

Combined Concrete Steel Frame (Model Validation)

Before trusting our nonlinear numerical models, we validated our modeling approach in OpenSees against an independent experimental benchmark: the study by Zhang, Harries, and Yuan on the seismic performance of hollow rectangular bridge piers, tested with and without steel fiber reinforced concrete. We replicated the geometry and loading protocol of their tested specimen, a hollow rectangular reinforced concrete column under a constant axial load and cyclic lateral displacement, using fiber-section elements in OpenSees, with the Concrete07 material model to capture unloading/reloading and post-crushing behavior of the concrete, and the Reinforcing Steel material model to capture strain hardening, buckling, and fracture behavior of the rebar. Comparing our numerically generated hysteresis loops with the experimental results showed excellent agreement: the peak base shear values differed by only 1.6% and 6.1% in the positive and negative loading directions respectively, and the overall shape, pinching behavior, and strength degradation trend of the loops matched closely, confirming that our modeling assumptions are reliable for the subsequent analysis of the actual ACC columns.

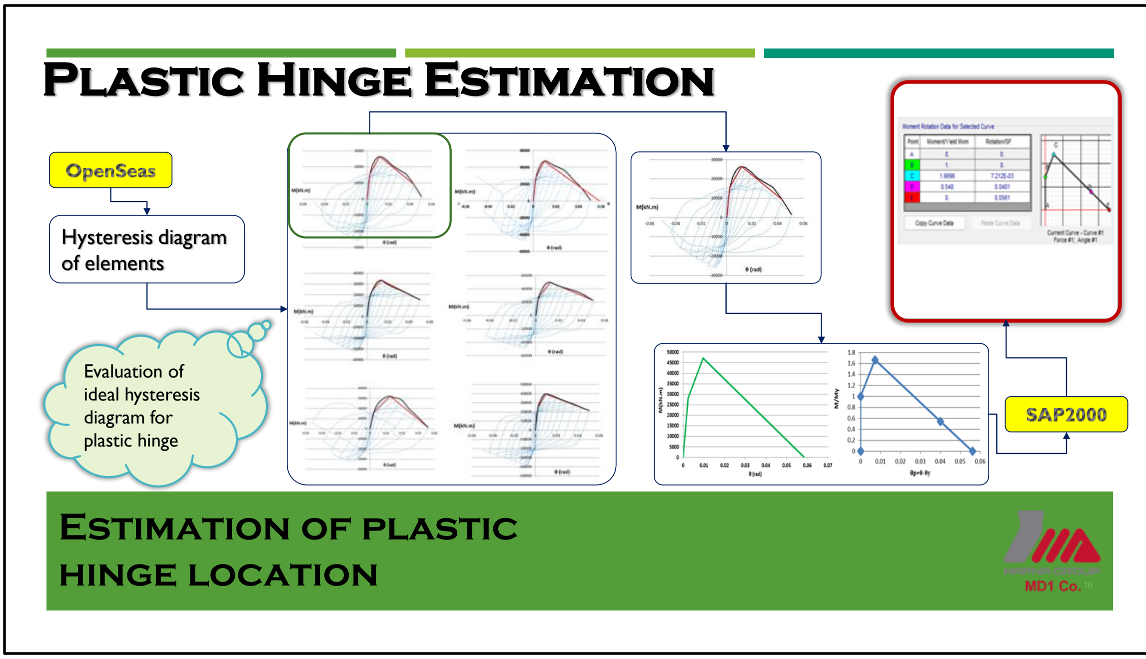

Combined Concrete Steel Frame (Plastic Hinge Estimation)
With the modeling approach validated, we proceeded to model each of the six distinct reinforced concrete column cross-sections identified across the eleven ACC structures individually in OpenSees, subjecting each to the same standardized cyclic loading protocol used in the validation study. From each column's resulting moment–rotation hysteresis diagram, we extracted an envelope curve and then idealized it as a piecewise-linear "backbone" curve, capturing the initial stiffness, yield point, and post-peak strength degradation, following the recommendations of ATC-72, which we found to provide more detailed and applicable guidance than FEMA 440 for this purpose. These idealized moment-rotation curves were then used to define the plastic hinge properties (in terms of moment ratio versus rotation, normalized by the yield values) that were assigned to the critical sections of each column in the SAP2000 structural models, enabling the software to capture nonlinear behavior even though it cannot natively handle full hysteretic curves.

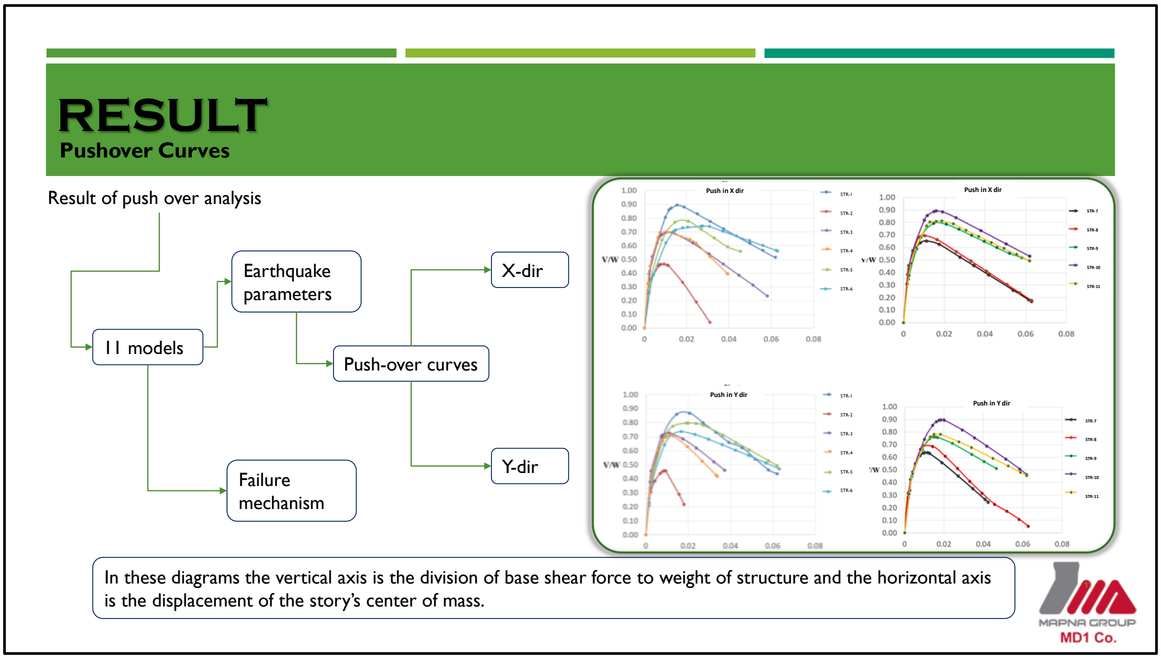

Result: Pushover Curves

Moving on to the results, for each of the eleven models, we performed nonlinear static pushover analysis independently in both the X and Y horizontal directions, applying a monotonically increasing lateral displacement at the center of mass of the roof/deck level, with P–Δ effects fully activated throughout. In total, this produced 22 pushover (capacity) curves. In these plots, the vertical axis represents the base shear normalized by the total structure weight (V/W), and the horizontal axis represents the lateral displacement of the deck's center of mass, normalized by the structure height. As you can see, the curves show a clear elastic branch, a peak capacity, and then a strength-degradation branch, which together form the basis for extracting the seismic design parameters and for identifying the sequence in which structural elements fail.

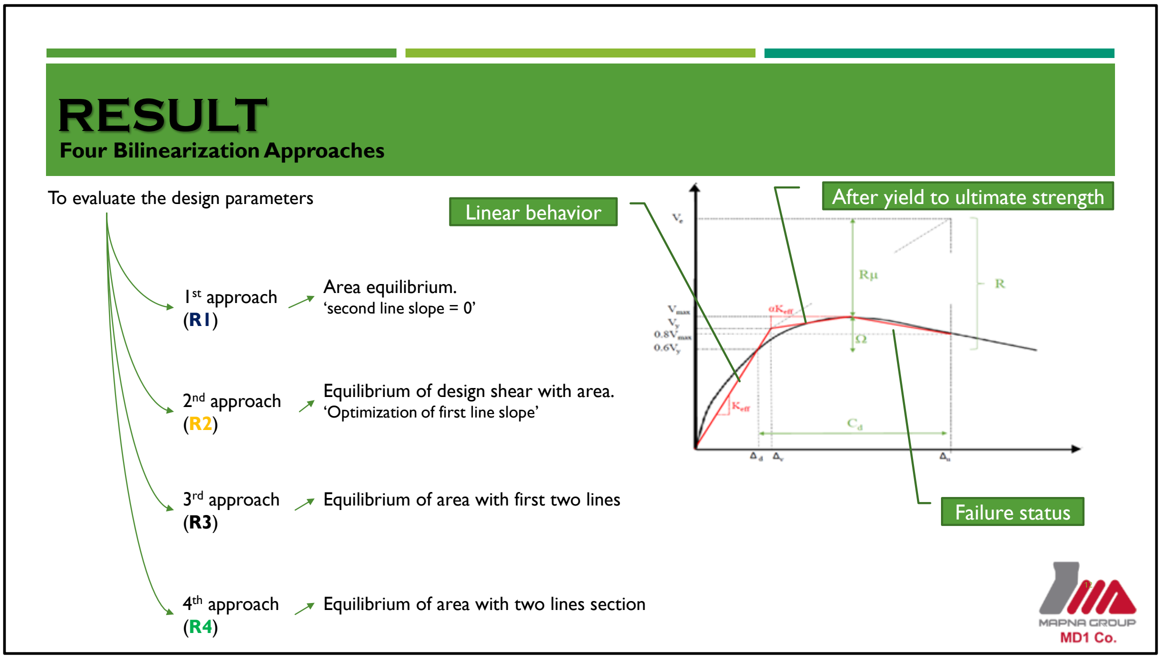

Result: Four Bilinearization Approaches

Since deriving design coefficients from a pushover curve requires idealizing it as a simplified bilinear or trilinear curve, and since this idealization process is inherently approximate and involves engineering judgment, we implemented and compared four different established approaches, consistent with FEMA 450 (NEHRP), FEMA 440, and ASCE 41-17. In the first approach, the post-yield line is drawn with zero slope and the areas under the idealized and actual curves are matched. In the second approach, the initial line's slope is optimized so it passes through the design-shear point on the actual curve, while the post-yield line's endpoint is fixed at 80% of peak base shear; areas are matched up to the design shear point. In the third approach, area equivalence is enforced only over the first two segments, the elastic branch and the immediate post-yield branch, up to their intersection point, placing emphasis on accurately capturing the elastic stiffness and the onset of yielding. In the fourth approach, area equivalence is enforced over the full bilinear portion of the idealized curve. From each idealized trilinear curve we then extract the response modification factor R, the ductility factor μ, and the overstrength factor Ω_0, following the standard definitions illustrated in the figure, based on the elastic strength demand Ve, the effective yield strength Vy, the maximum strength Vmax, and the corresponding displacements.

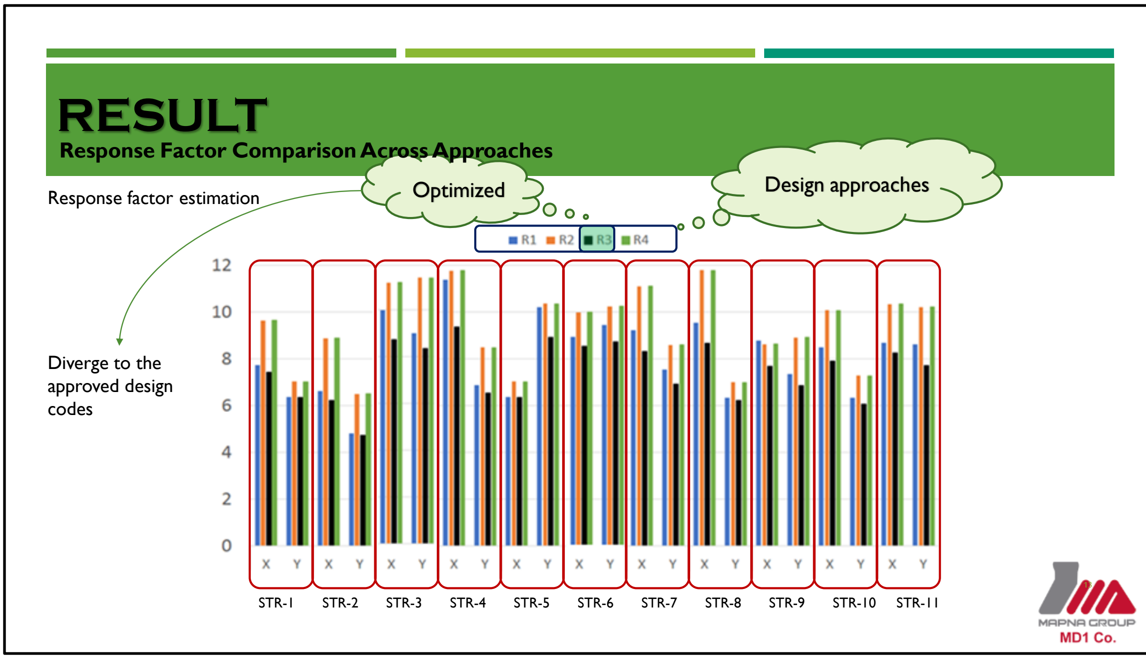

Result: Response Factor Comparison Across Approaches
When we compared the response modification factor values obtained from all four approaches across all eleven structures, a clear pattern emerged: approaches 1, 2, and 4 tend to systematically overestimate the response modification factor, producing values that diverge from the ranges recommended by established seismic codes for various structural systems. Approach 3, however, the one based on matching areas only over the initial elastic and early post-yield segments, produced the most reasonable and appropriately conservative estimates, showing much better convergence with the R-value ranges recommended in reputable design codes. Because of this closer agreement and its more conservative, safety-oriented outcome, we adopted approach 3 as the basis for computing all the seismic design coefficients reported as the final results of this study.

RESULT

Response Factor Comparison Across Approaches

R

Max = 9.37

Avrg = 7.49

Min = 4.74

R	Ω_0	μ	Model	
7.43	1.67	4.46	X	STR-1
6.34	1.67	3.8	Y	
6.23	1.67	3.74	X	STR-2
4.74	1.67	2.84	Y	
8.73	1.67	5.25	X	STR-3
8.34	1.67	5	Y	
9.35	1.67	5.61	X	STR-4
6.53	1.67	3.92	Y	
6.34	1.67	3.8	X	STR-5
8.93	1.67	5.36	Y	
8.54	1.67	5.13	X	STR-6
8.72	1.67	5.23	Y	
8.32	1.67	4.99	X	STR-7
6.91	1.67	4.15	Y	
8.68	1.67	5.21	X	STR-8
6.24	1.67	3.74	Y	
7.67	1.67	4.6	X	STR-9
6.86	1.67	4.11	Y	
7.91	1.67	4.74	X	STR-10
6.07	1.67	4.64	Y	
8.24	1.67	4.94	X	STR-11
7.72	1.67	4.63	Y	
7.49	1.67	4.50	Average	
1.17	0.00	0.71	Variance	

MAPNA GROUP
MD1 Co.

Result: Seismic Design Parameters Summary Table

This table summarizes the final seismic design coefficients, the response modification factor R, the overstrength factor Ω_0, and the ductility factor μ, obtained using approach 3, for each of the eleven structures in both the X and Y directions, giving 22 data points in total. Across all these cases, the response modification factor ranges from a minimum of 4.74 up to a maximum of 9.35, with an average of 7.49 and a standard deviation of about 1.17. The overstrength factor is remarkably consistent at 1.67 for every case, since it is governed directly by the fixed ratio between the design base shear and the code-specified elastic demand. The ductility factor averages 4.50, with a standard deviation of 0.71, reflecting good but somewhat variable deformation capacity across the different structural configurations. As shown earlier, more than 90% of the individual response modification factor values fall within the range of 6 to 9, which indicates a generally consistent and favorable energy-dissipation capacity across this family of structures.

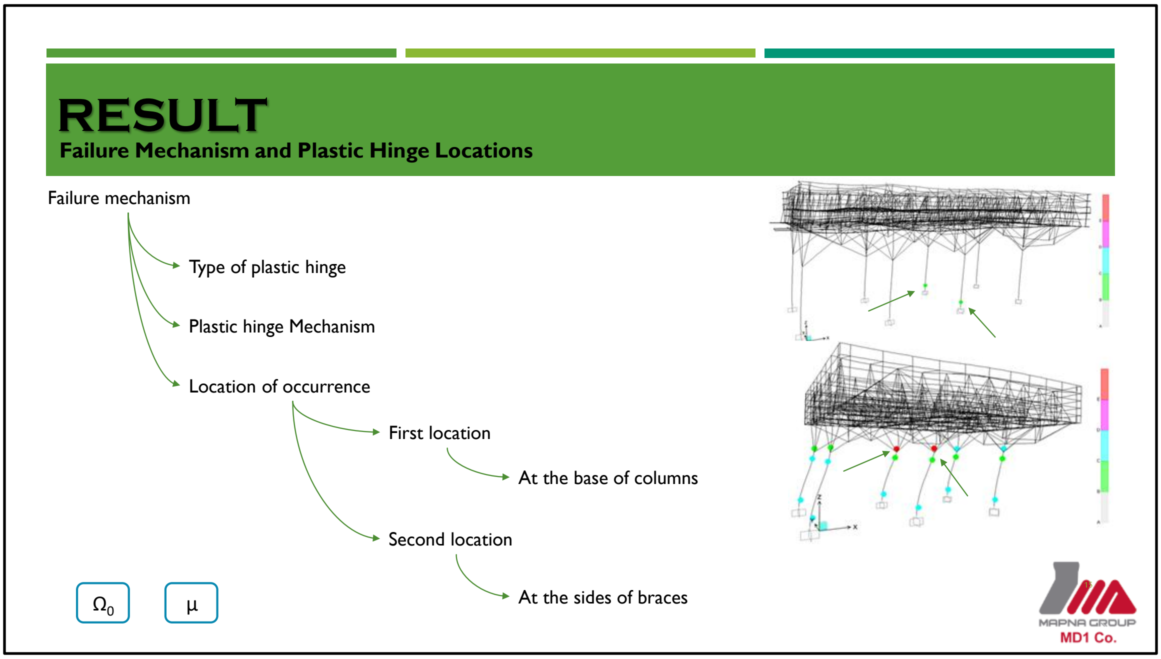

Result: Failure Mechanism and Plastic Hinge Locations

Now let's look at how and where damage develops in these structures. Tracking the formation and evolution of plastic hinges throughout the pushover analyses, in both the X and Y directions, we observed a consistent pattern: the very first plastic hinges always form at the base of a number of the reinforced concrete columns, near their foundation support, this is illustrated for Structures 2 and 4 in the paper. As the lateral load continues to increase, more columns develop base hinges, and at the same time, plastic hinges begin to form and spread at both the upper and lower ends of the brace-to-column connections. By the end of the pushover analysis, the hinges at the upper connection region between the braces and a number of columns reach the collapse/failure damage level, while hinges in other locations, including the column bases, remain at lower, less severe damage levels. This tells us that although damage initiates at the column bases, the upper brace-to-column connection region is actually the most critical location in terms of reaching structural failure, and therefore deserves special attention in detailing and design, since it plays a decisive role in controlling large deformations and maintaining overall structural stability.

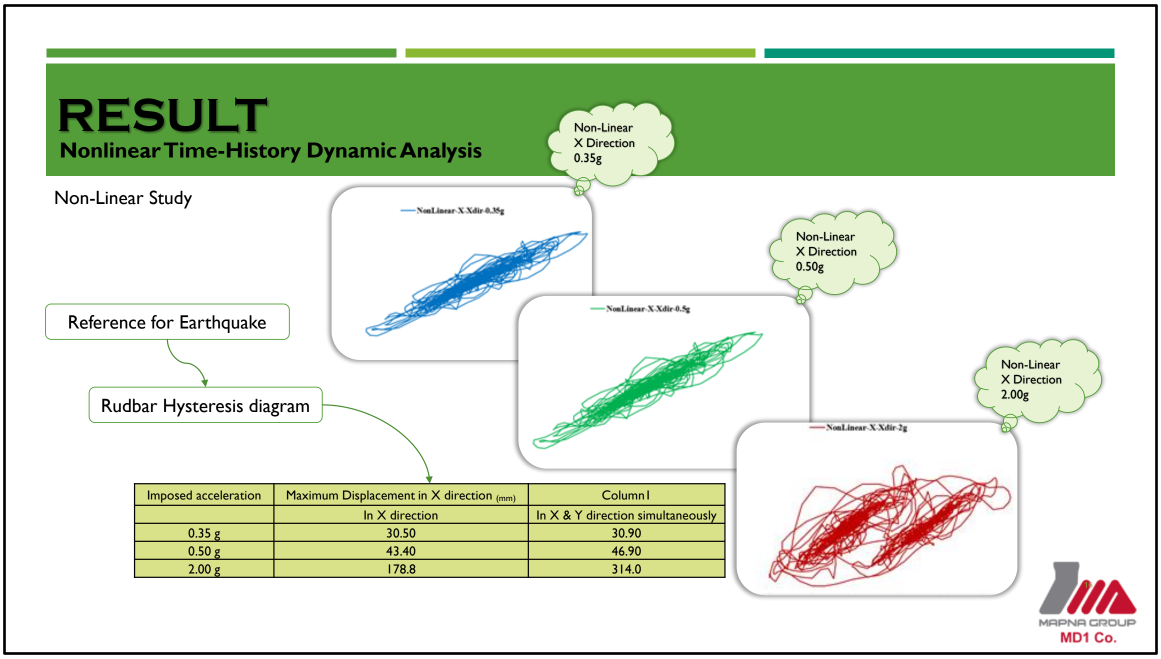

Result: Nonlinear Time-History Dynamic Analysis
To complement the static pushover results, we performed nonlinear time-history dynamic analysis on one representative model, Structure 2, using the recorded horizontal acceleration time-history from the Rudbar earthquake, scaled to three intensity levels: 0.35g, 0.5g, and 2.0g, corresponding respectively to the code Design Basis Earthquake (DBE), the Maximum Considered Earthquake (MCE), and a Collapse Prevention Earthquake (CPE) level. For each intensity level, we ran two separate analyses: one with the ground motion applied only in the X direction, and another with the X and Y components applied simultaneously. As the results table shows, the peak deck displacement in the X direction increases substantially with intensity, from about 30 mm at 0.35g, to roughly 45 mm at 0.5g, up to over 300 mm at 2.0g when both horizontal components act together. Notably, at the highest intensity level, applying both horizontal earthquake components simultaneously produced a significantly larger displacement and a hysteresis loop indicating greater energy absorption and more extensive nonlinear behavior than when only the X component was applied, confirming that bidirectional earthquake effects are important and should not be neglected in the design of these structures. It's also worth noting that under the single-direction record, damage concentrated most severely at the upper brace-to-column connection, whereas under the bidirectional record, comparable

damage severity was observed both at the column bases and at the brace connection regions.

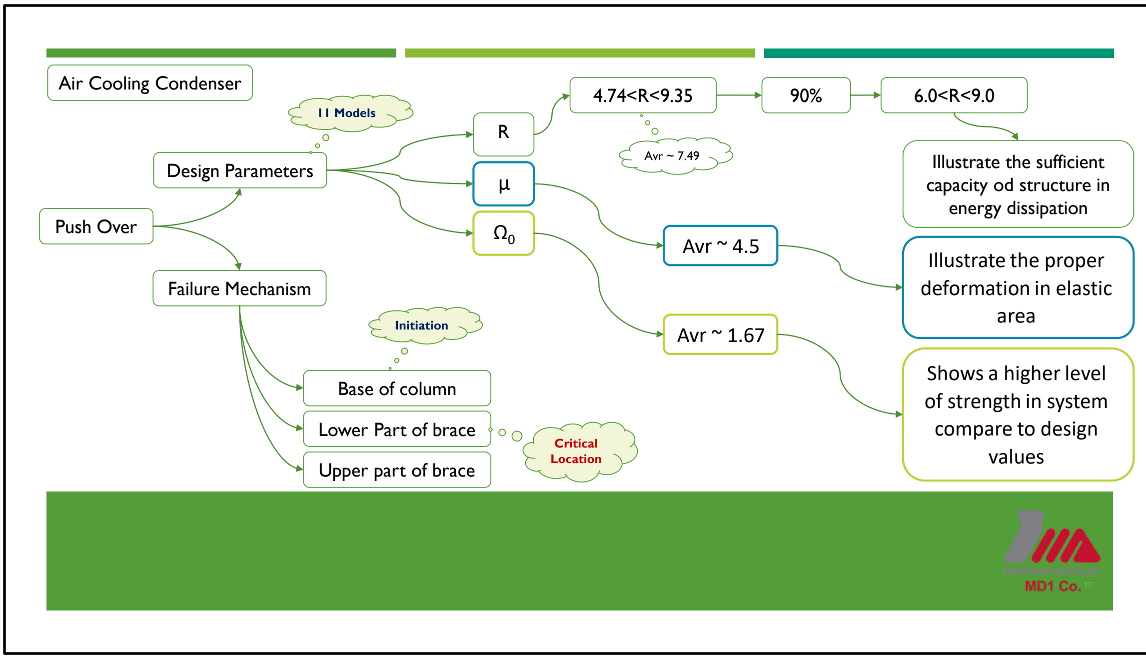

Summary Diagram / Conclusion

To conclude, let me summarize the overall picture. Based on pushover analysis of our eleven ACC support structure models, the response modification factor R ranges from 4.74 to 9.35, with more than 90% of values falling between 6 and 9 and an average around 7.49, this illustrates that these structures have sufficient capacity for seismic energy dissipation. The average ductility factor of about 4.5 illustrates that the structures can undergo proper, favorable deformation beyond the elastic range before failure. The average overstrength factor of about 1.67 shows that the system has a meaningful reserve of strength beyond the code-specified design values. Regarding the failure mechanism, damage initiates at the base of the concrete columns, but the truly critical locations, where damage is most likely to reach collapse levels, are at the lower and, especially, the upper parts of the brace-to-column connections. Taken together, these findings confirm that this composite concrete-steel system exhibits favorable seismic performance in terms of ductility, energy dissipation, and overstrength, while also highlighting the clear need to improve detailing and strengthen the brace-to-column connection region in order to enhance the seismic safety of similar structures in future power plant projects.

THANK YOU FOR YOUR ATTENTION

Thank you and I'd be happy to take any questions.